SPANDIDOS PUBLICATIONS EXPERIMENTAL AND THERAPEUTIC MEDICINE 15: 5199-5204, 2018

MRI manifestations of hepatic perfusion disorders

QING-YONG CAO[1], ZHI-MENG ZOU[1], QI WANG[1], CHUN-NI HE[1], QING ZOU[1] and BIN WANG[1,2]

[1]Department of Radiology, Yantai Affiliated Hospital of Binzhou Medical University;
[2]Medical Imaging Center, Binzhou Medical University, Yantai, Shandong 264100, P.R. China

Received December 14, 2015; Accepted January 6, 2017

DOI: 10.3892/etm.2018.6090

Abstract. The present study aimed to analyze the magnetic resonance imaging (MRI) results from patients with hepatic perfusion disorders (HPD) and liver diseases, in order to assess the pathogenetic mechanisms. This was completed byanalyzing the causes of HPD in 35 patients to assess if they were associated with arterioportal shunt, and classify the patients according to results from the MRI scans. Of the 35 patients, 26 (74.3%) with HPD presented with hepatocellular carcinoma, a major cause of HPD. The HPD phenomenon in 35 patients was not identified as obvious abnormal lesions on T2WI and T1WI according to the isointensity on diffusion weighted images. Enhanced scanning showed hyperintense signals on the arterial phase images, isointense or hyperintense signals on portal phase and delayed phase images. According to their MRI findings, hepatic perfusion disorders may be divided into different types, as follows: Diffuse, lobe or segment type, wedge type and platy. The HPD phenomenon may herald an underlying abnormality of liver disease and MRI may accurately diagnose HPDs in liver diseases.

Introduction

Hepatic perfusion disorder (HPD) refers to the difference in perfusion between a number of different liver segments and sub-segments induced by numerous causes, reflecting the partial liver microcirculation hemodynamic status (1). In 1997, Gryspeerdt *et al* (2) analyzed the phenomenon of hepatic perfusion differences identified in dual-phase spiral computed tomography (CT) scan, and first nominated the disorder as HPD. Following this identification of HPD, several studies concerning HPD have been published (3,4).

Etiopathogenesis of HPD is associcated with the certain imaging characteristics of HPD focal lesions, which are primarily categorized into three types: Diffuse type, liver lobe-liver segment type and wedge-sheet type (5). These diffuse types describe the multiple forms and various sizes of abnormal perfusion regions associated with HPD in the liver parenchyma. HPD is commonly observed in portal vein thrombosis and compression caused by malignant tumors (6). HPD liver lobe-liver segment type may be identified according to abnormally enhanced signals in the liver segment or liver lobe in the hepatic arterial phase and istypically observed in liver tumors or tumors of adjacent organs, post-liver surgery, interventional treatment or inflammatory lesions (4). The wedge-sheet type HPD is characterized by a wedge or triangular shape, which are commonly observed at the edge of the liver or liver lesions and are caused by liver cancer, cirrhosis, or abnormal physiological perfusion (7).

In China, the prevalence of liver disease is high, particularly those associated with viral hepatitis (predominantly hepatitis B virus), alcoholic liver disease and non alcoholic fatty liver disease, which affects ~300 million people (8). These diseases may progress into hepatic cirrhosis and liver cancer, which may result in HPD (9). Therefore, evaluation of HPD may help elucidate the hepatic pathological changes that occur in patients with HPD.

Following the extensive application of multislice computed tomography (MSCT), CT evaluations of HPD have previously been reported (10). However, few MRI evaluations of HPD have been reported, which is likely due to the fact that the use of MRI in imaging for evaulating HPD was introduced after CT and MRI is not used as widely as CT in imaging of HPD (11). However, the features of HPD in MRI imaging have been described in the literature (1), and it has been reported that MRI imaging maybe used to indicate the characteristics of different hepatic diseases that cause HPD (3). As the use of MRI has developed, it has been accepted in the medical community that MRI is superior to MSCT (10,12,13). Although the scanning speed of CT is fast, its soft-tissue resolution is lower than MRI (14). In addition, CT cannot be repeatedly performed in a the short term due to accumulation of radiation, whereas MRI does not harm the human body, thus repeated MRI may be deemed as safe to patients (15). MRI liver imaging can be completed in a short time period; regular enhanced MRI scanning of the liver can be done in 14 sec for each phase. In partitcular cases, the scanning speed of MRI can be shortened to several sec for each phase, and multi-phase scanning has been applied in evaluations of liver diseases (16). Furthermore, when assessing the liver and other abdominal lesions, more perfusion disorders may be identified using MRI scanning (3).

Correspondence to: Dr Qing-Yong Cao, Department of Radiology, Yantai Affiliated Hospital of Binzhou Medical University, 717 Golden Port Street, Muping, Yantai, Shandong 264100, P.R. China
E-mail: qingyongcaodoc@163.com

Key words: hepatic, perfusion, disorders, magnetic resonance imaging

In the present study, a retrospective analysis of 35 patients diagnosed with HPD through MRI in between January 2010 and January 2013 has been completed. The literature has been reviewed in order to enhance the awareness of HPD, improve the diagnosis of liver diseases and identify potential novel liver diseases (17).

Materials and methods

General information. A total of 35 patients with variation of HPD: 6 patients exhibtied diffuse type; 7 patients presented with liver lobe or liver segment type; and 22 patients had wedge or flaky type. Patients were diagnosed by unenhanced and dynamic contrast-enhanced MRI scanning in the Affiliated Hospital of Binzhou Medical College (Yantai, China) between January 2010 and January 2013 were selected for the current study. Among the 35 HPD patients, 26 were male and 9 were female; and the age of patients ranged from 41 to 82 years, with an average age of 59 years. Among these cases, there were 16 cases of liver cancer, 1 case of pancreatic cancer with hepatic metastasis, 1 case of hepatic hemangioma, 5 cases of hepatocellular carcinoma following interventional treatment, 1 case of liver cancer following surgery, 1 case of liver metastasis of colon cancer following radio frequency ablation, 1 case of gastric cancer, 3 cases of liver cirrhosis, 1 case of liver abscess, 1 case of cholecystitis and 1 case of pancreatitis. Primary lesions were not identified in 3 cases of radiological examination. All patients underwent plain MRI scanning, dynamic triple-phase enhanced scanning and ultrasound examination. Part of those cases underwent CT (7 cases), digital subtraction angiography (DSA, 5 cases), or needle biopsy (performed in 2 cases). DSA and needle biopsies were conducted according to previously described methods (18,19).

MRI examination. A Siemens MAGNETOM® Avanto 1.5T MR instrument (Siemens AG, Munich, Germany) was used to conduct examinations in the present study. A body phased-array coil was also used during examinations, where the phased array body coil was placed on the upper abdomen and close to the abdominal wall of the patient. All 35 patients underwent conventional T1 weighted image (WI), T2WI, fat saturation (FS) T2WI, FS T1WI, diffusion weighted images (DWI), dynamic contrast-enhanced imaging and delayed imaging. MRI imaging was performed as described previously (20). Patients were maintained in the supine position, in which the head entered the MRI machine first. High-resolution MRI imaging sequences include: T1WI repetition time (TR) 170 msec, echo time (TE) 4.8 msec, T2WI TR 1,200 msec, TE 92.0 msec; DWI b value was set to 50 and 600 sec/mm^2; FS T2WI TR 4,352 ms, TE 90 ms; FS T1WI1 acquisition matrix 512x512, field of view 380 mm, slice thickness 3 mm. The dynamic enhanced MRI scanning contrast agent was 20-25 ml gadolinium-diethylenetruamune pentaacetic acid. A scanning rate of 2 m/sec was used and the imaging time was as follows: Arterial phase 20-25 sec, portal venous phase 50-60 sec, delayed phase 120-180 sec. A total of 25 patients had a 5 min delay in imaging due to image changes.

MRI image viewing. Images were assessed by two experienced and specialized physicians in a blinded retrospective method. The occurrence of HPD was evaluated according to unenhanced and dynamic contrast-enhanced MRI imaging results at the same time, lesion size, and location, using the same enhancement pattern. The association between the HPD and lesions in the liver and abdomen was recorded, whether or not these were accompanied by an arterioportal shunt (APS). MRI, CT, DSA and related image data, laboratory tests, surgery and pathology results associated with the patient's primary lesions were comprehensively analyzed for the purpose of clarifying the causes of the diseases and provide an insight into the development mechanism of HPD.

MRI criteria that determined HPD were as follows: Abnormal perfusion regions in the arterial phase revealed a wedge or irregular hyperintense signal; the portal venous phase area revealed isointense or slightly hyperintense signals; the delayed phase imaging revealed isointense or hyperintense signals. According to its performance characteristics in the liver parenchyma, HPD may be classified as diffuse type, liver lobe-liver segment type, and wedges or flaky type.

The direct signs of APS to identify the patients with APS were as follows: i) Dynamic enhanced imaging in the arterial phase revealed intrahepatic portal vein branches, but the main portal vein did not appear; ii) Portal vein branches and trunk imaging appeared, but the superior mesenteric vein and splenic vein did not appear; iii) Signals within the proximal branches of the portal vein were markedly higher than within the distal branches.

Results

Patient information. Of all 35 HPD cases, 26 were tumor-related; accounting for 74.3% of the total number of cases assessed, which included 16 cases of primary liver cancer, 1 case of liver metastases, 1 case of hepatic hemangioma, 1 case of gastric cancer, 6 cases of hepatocellular carcinoma following surgery and interventional treatment and 1 case of liver metastases following treatment intervention. There were 6 non-tumor associated cases, accounting for 17.1% of total HPD cases including 3 cases of inflammatory lesions and 3 cases of liver cirrhosis while 10 cases of APS HPD were identified. Therefore, tumor-associated lesions account for a relatively large amount of HPD cases in the group in the present study. Primary liver cancer is a common malignant tumor that seriously threatens human health globally, as the sixth most lethal malignant tumor (21) and is the most common disease that causes HPD. Furthermore, inflammatory lesions and non-neoplastic causes of cirrhosis are common causes of HPD (22,23). Transcatheter arterial chemoembolization (TACE) is the primary measurement approach of interventional treatment for liver cancer (24). Interventional therapy typically leads to HPD (25). Clear primary lesions were not identified in three of the cases presented in the current study, which were considered to physiologically cause HPD; accounting for 8.6% of HPD cases. Pathogenic causes and the different types of HPD are presented in Table I.

Comparison of MRI and CT in HPD imaging. Of the 35 HPD cases assessed, 7 also underwent plain CT and 3 underwent enhanced scan imaging. Furthermore, 6 of the 35 cases underwent CT scan imaging, which revealed abnormal perfusion

Table I. Pathogenic causes and different types of hepatic perfusion disorders of 35 patients.

Pathogenic cause	Diffuse type	Liver lobe and segment type	Wedge-shaped type	Total
Liver cancer	3	1	12	16
Following liver cancer treatment	1	2	4	7
Hepatic hemangioma			1	1
Hepatic metastasis	1			1
Gastric cancer		1		1
Cirrhosis		1	2	3
Liver abscess		1		1
Cholecystitis		1		1
Pancreatitis	1			1
Physiology			3	3
Total	6	7	22	35

regions with a marked enhancement in the arterial phase and signals in balanced and delayed phases that appeared near the liver parenchyma; the performance of the CT scanning images appear to be similar to MRI enhanced imaging. Atypical signs were observed in 1 case of HPD that underwent CT scanning. This may be associated with the rate of contrast agents and different imaging modalities. As noted previously, MRI has a number of advantages in displaying HPD.

MRI imaging of patients. Fig. 1 indicated the MRI imaging of a patient (male, with a history of hepatitis B) with liver cell adenocarcinoma revealed by biopsy. Fig. 1A-C demonstrated the imaging of the tumor. Fig. 1A indicated the tumor in the arterial phase was markedly enhanced. Fig. 1B demonstrated that the signal of the tumor in the venous phase was slightly hyperintense, while in the delayed phase the tumor displayed hypointense signals (Fig. 1C). Fig. 1D-F demonstrated the imaging of abnormal perfusion in the liver inferior to the adjacent region. Abnormal perfusion in the arterial phase was hyperintense (Fig. 1D). Furthermore, abnormal perfusion in the venous phase and the delayed phase was also slightly hyperintense (Fig. 1E and F, respectively).

Fig. 2 indicated the liver enhanced MRI imaging of a patient with cholecystitis. Imaging in the arterial phase demosntrated multiple abnormal enhancements in the left and right lobe of the liver with clear boundaries (Fig. 2A). In the portal phase, abnormalities in the left and right lobe of the liver were slightly hyperintense (Fig. 2B). Notably, abnormalities in the left and right lobe of the liver in the delayed phase were also slightly hyperintense (Fig. 2C).

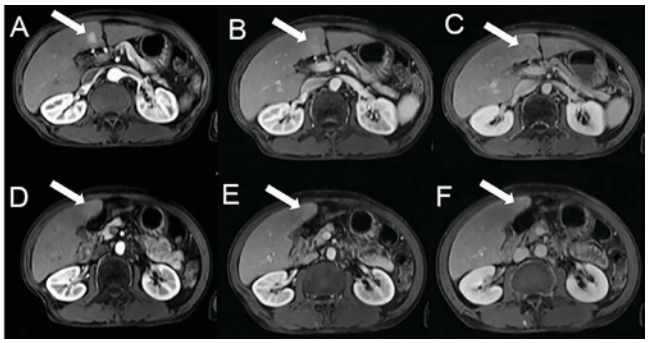

Figure 1. Surrounding liver tissue perfusion disorders caused by liver cancer of a male, aged 62, with history of hepatitis B. White arrow in each panel indicated the tumor in the liver. (A) Imaging in the arterial phase was significantly enhanced. (B) Imaging in the venous phase is slightly hyperintense. (C) Imaging in the delayed phase indicates hypointense signals. Biopsy reveals liver cell adenocarcinoma and abnormal perfusion in the liver inferior to the adjacent region. (D) Imaging in the arterial phase was hyperintense. (E) Imaging in the venous phase and (F) delayed phase is slightly hyperintense.

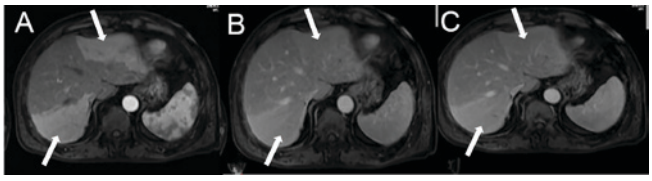

Figure 2. Case of liver tissue perfusion disorder caused by cholecystitis in a male aged 70, with history of cholecystitis and hepatic perfusion disorder. The upper and lower white arrows in each panel indicate the two hepatic perfusion disorder areas, which were all liver lobe-liver segment type. Liver enhanced imaging (A) in the arterial phase indicates multiple abnormal enhancements in the left and right lobe of the liver with clear boundaries. (B) Imaging in the portal phase and (C) delayed phase was slightly hyperintense.

Discussion

MRI scanning of HPD primarily indicates isointense T1 and T2 signals. A previous study reported that HPD may exhibit long T1 and T2 signals (17). In all 35 cases, the plain MRI scan revealed isointense-T1 and isointense-T2 signals, as well as isointense-DWI signals; when cases underwent an enhanced scan. HPD primarily appeared as a transient wedge, triangular, oval-shaped or an abnormal enhancement zone in the arterial phase. Signals were isointense with sharp edges, which demonstrate a clear narrow transition zone with the surrounding liver tissue. Furthermore, there was no vasculature displacement, blood vessel signals were observed within high-perfusion abnormal signals and isointense or slightly hyperintense signals were observed in the portal venous phase and delayed phase. The segment and sub-segment of the liver

and liver lobe may be affected and can be single or multiple sites, which are primarily located in the peripheral region of the liver (26).

According to its performance characteristics in the liver parenchyma, HPD may be divided into three types (5): i) The diffuse type: Presents with multiple forms, numerous sizes of abnormal perfusion regions in the liver parenchyma; exhibits irregular hyperintense abnormal enhancement signals, patchy or round in the arterial phase. In the present study, 6 cases were determined to be this type, which are common in malignant tumor portal vein thrombosis and compression. ii) Liver lobe-liver segment type: Exhibits abnormal enhanced signals in the liver segment or liver lobe in the hepatic arterial phase (27). In the present study, 7 cases were identified to be this type, which are commonly observed in liver tumors or adjacent organ tumors (28), post-liver surgery or interventional treatment (4). or in inflammatory lesions (29). iii) Wedge-sheet type: Abnormal perfusion regions present a wedge or sheet shape, which are commonly observed at the edge of the liver or liver lesions. In the present study, 22 cases belonged to this type, which are commonly observed in liver cancer, cirrhosis and abnormal physiological perfusion (30,31). Danet *et al* (32) reported that in 16 cases of pancreatic cancer liver metastasis enhanced MRI scans, 8 cases (50%, 8/16) revealed a wedge enhancement. In the present study, in the 16 patients with liver cancer, 12 cases (75%) indicated wedge-sheet type HPD, which higher than the rate indicated in the study by Danet *et al* (32), indicating that the present results were consistent with these previous findings. Furthermore, these findings suggest that the wedge-sheet typemay be a typical characteristic for HPD caused by liver cancer.

HPD with atypical performance often requires the identification of hepatocellular carcinoma, liver metastases, liver hemangioma, focal nodular hyperplasia, hepatic adenoma and hepatic tumor recurrence following the treatment of differentiated lesions (33). Hepatocellular cancer primarily manifests as long T1 and T2 signals, while DWI demonstrates high signals in enhanced scanning imaging (34). High signals were observed in the arterial phase, while the delayed phase exhibited low signals (35). Metastatic tumors demonstrate complex signal changes, while typical liver metastases exhibit a T2WI 'target sign' or 'bull's-eye' sign (36). In the portal phase, enhanced scanning revealed a loop-shaped enhancement. Hypointense T1WI signals and hyperintense T2WI signals primarily demonstrate hemangiomas, while enhanced scans revealed progressive enhancements. The presence of focal nodular hyperplasia was determined by isointense or slightly hypointense T1WI signals and slightly hyperintense or isointense T2WI signals. In the central scar, T2WI hyperintense signals were observed. In the early stage of enhanced scanning, significantly enhanced signals were observed and slightly hyperintense signals were observed in the late stage. In the central scar, delayed enhancement was demonstrated. Solitary round shapes were primarily observed in the liver adenoma, T1WI signals may be slightly hyperintense or hypointense and T2WI revealed slightly hyperintense signals. In enhanced scans, a significant enhancement was demonstrated in the arterial phase, while the portal and delayed phases revealed isointense and hypointense signals or isointense and hyperintense signals. The recurrence of tumors following treatment typically indicates long T1 and T2 signals (37). In enhanced scans, enhancement signals are observed in the arterial phase, while decreased signals are observed in the delayed phase. DWI presents with hyperintense signals and thus, these were identified as HPD (26). In DWI, by evaluating the microscopic motion of water molecules within living tissues, it is possible to detect functional changes in tumor tissues following TACE surgery in the early stages of cancer (38). Previous studies have indicated that DWI is expected to become an effective means of determining efficacy, as well as the post-surgery follow-up assessment of liver cancer TACE therapy (39). In order to understand the effect of interventional therapy, important reference information for the follow-up treatment of patients is required (40).

Anatomic variations of hepatic artery constitutes a 'third hepatic inflow tract' that primarily occurs in: The gallbladder fossa, the attachment point of the ligament, front side of the porta hepatis, the front margin of the II segment, front and rear margins of the III segment and specific parts of the liver subcapsular region (41). In the early arterial phase of liver CT and MRI enhanced scans, the contrast agent and reflux of the portal vein through the spleen and gastrointestinal tract have not been fully and uniformly mixed; thus, abnormal physiological hypoperfusion of the liver may occur (42).

Mechanisms of abnormal pathological hyper perfusion are complex and are summarized as follows (2): i) This may occur due to trauma, a number of different invasive procedures., including after liver tumor interventional therapy, or following liver transplantation (43). ii) Tumors, including benign and malignant liver tumors (26), the incidence of HPD in primary liver cancer is 6.4 to 21% (44) and Kim *et al* (45) reported that the incidence of HPD in liver hemangiomas was 25.7%. iii) Inflammation; inflammatory diseases in the liver and adjacent organs such as liver abscess, cholangitis and cholecystitis (23); abnormal perfusion phenomenon of round lesions or near the liver parenchyma associated with liver abscess has been reported (46) and is considered an important diagnostic indication of liver abscess (47). iv) Compressed or blocked blood vessels within the liver: The hepatic portal vain is the most commonly involved (42); portal vein obstruction, portal vein tumor thrombus or direct compression of the portal vein by tumors that lead to reduced blood flow and blood supply via the hepatic artery is increased to compensate (25).

The most common cause for this is a compressed or blocked liver artery, hemodynamic balance between hepatic artery and portal vein changes and reduction in perfusion of the affected liver or hepatic artery (22); thus, inducing liver pathologic hypoperfusion abnormalities (48).

HPD in specific regions and other parts of the gallbladder fossa, when other reasons are excluded, may suggest the presence of a third inflow tract without prompting any pathological significance. HPD in simple imaging should not be considered as a simple hemodynamic change and should lead to clinical attention and regular follow-ups, if necessary. Biopsy should be conducted to exclude or diagnose the true disease and to avoid misdiagnosis or missed diagnosis.

The difference between APS dynamic portal pressure observed in the patients may be relatively large, and portal vein branches that present early may be observed in the arterial phase. Certain dynamic portal pressure differences

are relatively small, and it is not easy to identify portal vein branches that present early. The presence or absence of APS is significant for determining an intervention treatment plan. Liver cirrhosis may lead to reduced portal vein perfusion and increased compensatory hepatic artery perfusion; thus, causing HPDs (49). APS is commonly identified in cirrhosis, with an angiographic detection rate of 13% (42). However, the MRI detection rate is relatively low and definite APS was not detected in three cases of cirrhosis in the current study.

HPD may be an indirect sign of true lesions, since early intrahepatic metastasis affects small liver blood vessel branches. Imaging cannot exhibit direct metastatic lesions, and may only present as HPD. Over time, metastasis may develop and larger lesions may form. Thus, early intrahepatic metastasis in patients with cancer who exhibit signs of HPD away from the main tumor foci should be given attention.

Certain extra-hepatic adjacent organs such as the stomach, pancreas, kidneys or retroperitoneal tumors may induce hemodynamic changes in the portal vein and hepatic artery when they violate extra-hepatic portal vein branches, celiac or the inferior vena cava; which lead to liver perfusion differences and present HPD.

In conclusion, HPD induced by liver cancer and other causes, including cirrhosis, hemangioma, inflammation and adjacent viscera lesions, is not uncommon. HPD does not have a characteristic diagnostic value for liver lesions, but it may indicate the presence of abnormal hepatic arterial blood flow, portal vein obstruction or artery-portal vein shunt and other potential pathological changes. Dynamic contrast-enhanced MRI imaging is sensitive to HPD and is able to detect small liver lesions and artery-portal vein diversion, as well as in detecting occult lesions. However, further studies are required to establish suitable methods for the detection and evaluation of HPD using MRI imaging.

Acknowledgements

The present study was funded by the National Natural Science Foundation of China (grant nos. 81171303 and 30470518), Development Project of Health and Science and Technology (grant nos. 2011WSB29009 and 2011HW067) and the Department of Shandong Province Outstanding Academic Leaders Fund of the Health System of Shandong Province (grant no. 2006-39).

References

1. Tian JL and Zhang JS: Hepatic perfusion disorders: Etiopathogenesis and related diseases. World J Gastroenterol 12: 3265-3270, 2006.
2. Gryspeerdt S, Van Hoe L, Marchal G and Baert AL: Evaluation of hepatic perfusion disorders with double-phase spiral CT. Radiographics 17: 337-348, 1997.
3. Lupescu IG, Grasu M, Capsa R, Pitrop A and Georgescu SA: Hepatic perfusion disorders: Computer-tomographic and magnetic resonance imaging. J Gastrointestin Liver Dis 15: 273-279, 2006.
4. Quiroga S, Sebastià C, Pallisa E, Castellà E, Pérez-Lafuente M and Alvarez-Castells A: Improved diagnosis of hepatic perfusion disorders: Value of hepatic arterial phase imaging during helical CT. Radiographics 21: 65-81; Questionnaire 288-294, 2001.
5. Colagrande S, Centi N, La Villa G and Villari N: Transient hepatic attenuation differences. AJR Am J Roentgenol 183: 459-464, 2004.
6. Zhou X, Luo Y, Peng YL, Cai W, Lu Q, Lin L, Sha XX, Li YZ and Zhu M: Hepatic perfusion disorder associated with focal liver lesions: Contrast-enhanced US patterns-correlation study with contrast-enhanced CT. Radiology 260: 274-281, 2011.
7. Colagrande S, Centi N, Carmignani L, Salvatore Politi L and Villari N: Meaning and etiopathogenesis of sectorial transient hepatic attenuation differences (THAD). Radiol Med 105: 180-187, 2003 (In Italian).
8. Wang FS, Fan JG, Zhang Z, Gao B and Wang HY: The global burden of liver disease: The major impact of China. Hepatology 60: 2099-2108, 2014.
9. Byun JH, Kim TK, Lee CW, Lee JK, Kim AY, Kim PN, Ha HK and Lee MG: Arterioportal shunt: Prevalence in small hemangiomas versus that in hepatocellular carcinomas 3 cm or smaller at two-phase helical CT. Radiology 232: 354-360, 2004.
10. Hwang J, Kim SH, Lee MW and Lee JY: Small (≤2 cm) hepatocellular carcinoma in patients with chronic liver disease: Comparison of gadoxetic acid-enhanced 3.0 T MRI and multiphasic 64-multirow detector CT. Br J Radiol 85: e314-e322, 2012.
11. Imai Y, Katayama K, Hori M, Yakushijin T, Fujimoto K, Itoh T, Igura T, Sakakibara M, Takamura M, Tsurusaki M, *et al*: Prospective comparison of Gd-EOB-DTPA-enhanced MRI with dynamic CT for detecting recurrence of HCC after radiofrequency ablation. Liver Cancer 6: 349-359, 2017.
12. Park MJ, Kim YK, Lee MW, Lee WJ, Kim YS, Kim SH, Choi D and Rhim H: Small hepatocellular carcinomas: Improved sensitivity by combining gadoxetic acid-enhanced and diffusion-weighted MR imaging patterns. Radiology 264: 761-770, 2012.
13. Yang JZ, Huo YJ, Zhang Y, Yuan J, Yang FY and Zhao YQ: Experience of 3.0T MRI detection and diagnosis of <1.0 cm small hepatocellular cancer. J Pract Radiol: 30, 2014 (In Chinese).
14. Tang A, Cruite I and Sirlin CB: Toward a standardized system for hepatocellular carcinoma diagnosis using computed tomography and MRI. Expert Rev Gastroenterol Hepatol 7: 269-279, 2013.
15. Mirsadraee S and van Beek EJ: Functional imaging: Computed tomography and MRI. Clin Chest Med 36: 349-363, x, 2015.
16. Marolf AJ: Computed tomography and MRI of the hepatobiliary system and pancreas. Vet Clin North Am Small Anim Pract 46: 481-497, vi, 2016.
17. Chen SL, Cao LR, Ji SZ and Liu M: The MRI manifestations of hepatic perfusion disorders in focal liver lesions. J Pract Radiol, 2009 (In Chinese).
18. Yan SX, Liang TB, Fujii M, Kawamitsu H, Sugimura K and Zheng SS: Modified magnetic resonance angiography of the liver using sensitivity encoding in comparison with digital subtraction angiography and CT arterial portography. Hepatobiliary Pancreat Dis Int 4: 185-191, 2005.
19. Amédée-Manesme O, Furr HC and Olson JA: The correlation between liver vitamin A concentrations in micro-(needle biopsy) and macrosamples of human liver specimens obtained at autopsy. Am J Clin Nutr 39: 315-319, 1984.
20. Rofsky NM, Lee VS, Laub G, Pollack MA, Krinsky GA, Thomasson D, Ambrosino MM and Weinreb JC: Abdominal MR imaging with a volumetric interpolated breath-hold examination. Radiology 212: 876-884, 1999.
21. Dong S, Ye XD, Yuan Z, Xu LC and Xiao XS: Relationship of apparent diffusion coefficient to survival for patients with unresectable primary hepatocellular carcinoma after chemoembolization. Eur J Radiol 81: 472-477, 2012.
22. Wang BZ and Yang HX: CT findings and formation mechanism of hepatic abnormal perfusion. Inner Mongolia Med J 2: 3, 2011.
23. Luo GZ, Huang LM and Zou W: Liver transient perfusion abnormalities in spiral CT diagnosis of acute cholecystitis. Hunan Med 25: 3, 2014 (In Chinese).
24. Vilgrain V: Advancement in HCC imaging: diagnosis, staging and treatment efficacy assessments: Hepatocellular carcinoma: Imaging in assessing treatment efficacy. J Hepatobiliary Pancreat Sci 17: 374-379, 2010.
25. Kim HJ, Kim AY, Kim TK, Byun JH, Won HJ, Kim KW, Shin YM, Kim PN, Ha HK and Lee MG: Transient hepatic attenuation differences in focal hepatic lesions: Dynamic CT features. AJR Am J Roentgenol 184: 83-90, 2005.
26. Zhou KG and Chen ZW: Body magnetic resonance imaging. Shanghai Med Univ Press: 4, 2009.
27. Tan Y and Yang ZH: Multislice spiral CT evaluation for anormal peripheral perfusion of hepatic hemangioma. J Clin Radiol, 2008 (In Chinese).
28. Itai Y and Matsui O: Blood flow and liver imaging. Radiology 202: 306-314, 1997.

29. Arai K, Kawai K, Kohda W, Tatsu H, Matsui O and Nakahama T: Dynamic CT of acute cholangitis: Early inhomogeneous enhancement of the liver. AJR Am J Roentgenol 181: 115-118, 2003.
30. Yu YM, Cui Y and Wang YX: Preliminary application of 128-slice 4D CT whole-liver perfusion imaging in hepatocellular carcinoma. Chin Imaging J Integr Tradit West Med 9: 3, 2011 (In Chinese).
31. Li XH, Mo HM and Guo PX: Relationship between liver perfusion imaging of CT and severity of hepatic cirrhosis. Chin Imaging J Integr Tradit West Med 8: 3, 2010 (In Chinese).
32. Danet IM, Semelka RC, Nagase LL, Woosely JT, Leonardou P and Armao D: Liver metastases from pancreatic adenocarcinoma: MR imaging characteristics. J Magn Reson Imaging 18: 181-188, 2003.
33. Van Beers BE, Leconte I, Materne R, Smith AM, Jamart J and Horsmans Y: Hepatic perfusion parameters in chronic liver disease: Dynamic CT measurements correlated with disease severity. AJR Am J Roentgenol 176: 667-673, 2001.
34. Lee MJ, Saini S, Compton CC and Malt RA: MR demonstration of edema adjacent to a liver metastasis: Pathologic correlation. AJR Am J Roentgenol 157: 499-501, 1991.
35. Brodsky EK, Bultman EM, Johnson KM, Horng DE, Schelman WR, Block WF and Reeder SB: High-spatial and high-temporal resolution dynamic contrast-enhanced perfusion imaging of the liver with time-resolved three-dimensional radial MRI. Magn Reson Med 71: 934-941, 2014.
36. Ferrucci JT: Liver tumor imaging: Current concepts. AJR Am J Roentgenol 155: 473-484, 1990.
37. Harned RK II, Chezmar JL and Nelson RC: Imaging of patients with potentially resectable hepatic neoplasms. AJR Am J Roentgenol 159: 1191-1194, 1992.
38. Chen CY, Li CW, Kuo YT, Jaw TS, Wu DK, Jao JC, Hsu JS and Liu GC: Early response of hepatocellular carcinoma to transcatheter arterial chemoembolization: Choline levels and MR diffusion constants-initial experience. Radiology 239: 448-456, 2006.
39. Ma XH and Zhou C: Progress of diffusion-weighted imaging and perfusion-weighted imaging in evaluation on therapeutic efficiency of transcatheter arterial chemoembolization of hepatocellular carcinoma. J Int Med Radiol 36: 344-348 2013 (In Chinese).
40. Kim HH, Kim JC, Park EK, Hur YH, Koh YS, Cho CK, Kim HS and Kim HJ: Undifferentiated embryonal sarcoma of the liver presenting as a hemorrhagic cystic tumor in an adult. Hepatobiliary Pancreat Dis Int 10: 657-660, 2011.
41. Ikeda O, Tamura Y, Nakasone Y, Shiraishi S, Kawanaka K, Tomiguchi S, Yamashita Y, Takamori H, Kanemitsu K and Baba H: Comparison of intrahepatic and pancreatic perfusion on fusion images using a combined SPECT/CT system and assessment of efficacy of combined continuous arterial infusion and systemic chemotherapy in advanced pancreatic carcinoma. Cardiovasc Intervent Radiol 30: 912-921, 2007.
42. Colagrande S, Carmignani L, Pagliari A, Capaccioli L and Villari N: Transient hepatic attenuation differences (THAD) not connected to focal lesions. Radiol Med 104: 25-43, 2002 (In English, Italian).
43. Wang J, He BJ, Liao BH, Jiang ZB, Luo L, Zhang YQ, Chen GH, Yang Y and Shan H: MRI diagnosis of liver grafts complications after liver transplantation. Chin Med Imaging Technol 27: 997-1000, 2011 (In Chinese).
44. Giovagnoni A, Terilli F, Ercolani P, Paci E and Piga A: MR imaging of hepatic masses: Diagnostic significance of wedge-shaped areas of increased signal intensity surrounding the lesion. AJR Am J Roentgenol 163: 1093-1097, 1994.
45. Kim KW, Kim TK, Han JK, Kim AY, Lee HJ and Choi BI: Hepatic hemangiomas with arterioportal shunt: Findings at two-phase CT. Radiology 219: 707-711, 2001.
46. Balci NC, Semelka RC, Noone TC, Siegelman ES, de Beeck BO, Brown JJ and Lee MG: Pyogenic hepatic abscesses: MRI findings on T1- and T2-weighted and serial gadolinium-enhanced gradient-echo images. J Magn Reson Imaging 9: 285-290, 1999.
47. Colagrande S, Centi N, Galdiero R and Ragozzino A: Transient hepatic intensity differences: Part 1, Those associated with focal lesions. AJR Am J Roentgenol 188: 154-159, 2007.
48. Qin GD: Liver perfusion abnormalities imaging findings and mechanisms. Chin Contemp Med 34, 2012 (In Chinese).
49. Choi BI, Lee KH, Han JK and Lee JM: Hepatic arterioportal shunts: Dynamic CT and MR features. Korean J Radiol 3: 1-15, 2002.